

Cite this: *Chem. Sci.*, 2024, 15, 13240

All publication charges for this article have been paid for by the Royal Society of Chemistry

Enantioconvergent and diastereoselective synthesis of atropisomeric hydrazides bearing a cyclic quaternary stereocenter through ternary catalysis†

Xia Wang,^a Shao-Jie Wang,^a Xiaolan Xin,^a Hao An,^a Zhifeng Tu,^{*a} Hui Yang,^{id b} Ming Wah Wong^{id *b} and Shenci Lu^{id *a}

An efficient and highly enantioconvergent and diastereoselective ternary catalysis in a one-pot process is reported, which represents an integrated strategy for the synthesis of atropisomeric hydrazides with defined vicinal central and axial chirality from readily available racemic α -amino-ynones, azodicarboxylates, and Morita–Baylis–Hillman (MBH) carbonates. This method utilizes *in situ*-generated racemic pyrrolin-4-ones *via* hydroamination of racemic α -amino-ynones by AuCl catalysis as a novel and versatile C1 synthon, which engage commercially available azodicarboxylates to generate amination products in high yields and uniformly excellent enantioselectivities under the catalysis of a chiral phosphoric acid. Following amination, *N*-alkylation catalyzed by diastereoselective organocatalyst afforded axially chiral hydrazides with excellent diastereoselectivities (>98 : 2 dr). The synthetic utility of the amination products and axially chiral hydrazides was also demonstrated by their facile conversion to diverse molecules in high yields with excellent stereopurity. Density functional theory calculations were performed to understand the origin of diastereoselectivity.

Received 15th May 2024
Accepted 27th June 2024

DOI: 10.1039/d4sc03190c

rsc.li/chemical-science

Introduction

One emerging strategy for synthesizing complex chiral molecules is to use multiple catalysts to promote asymmetric tandem reactions, which features sequential activation of the starting materials or *in situ*-generated intermediates, with high levels of step- and atom-economy.¹ Remarkable advances have been made with asymmetric cascade reactions using three combinations of two distinct catalysts (*i.e.*, metal/metal, metal/organo, and organo/organo). These combinations enable enantio- and diastereoselective asymmetric ternary catalysis; however, the methods are quite limited.² As illustrated in Scheme 1a, where ternary catalysis is shown to be a cascade process in which three catalytic cycles are involved, intermediate I is formed in the first catalytic transformation and engages in the second catalyzed reaction to afford intermediate II. This is then subjected to a third catalyzed transformation to

deliver molecular complexity from simple starting materials. Racemic pyrrolin-4-one, which is easily accessed from readily available racemic α -amino-ynones under gold catalysis,³ may serve as a highly effective nucleophilic synthon for the ternary catalytic reaction. However, the functionalization of pyrrolin-4-ones using this strategy remains elusive (see Scheme 1b).

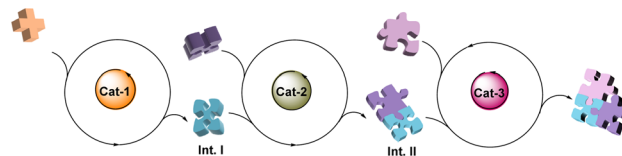
The hydrazides are a class of highly valuable compounds. Some hydrazides, such as aza-peptide analog CGP 53820, are bioactive molecules, exhibiting potent inhibition of HIV-1 and HIV-2 protease. Others are used in environmentally benign

^aFrontiers Science Center for Flexible Electronics (FSCFE), Shaanxi Institute of Flexible Electronics (SIFE), Shaanxi Institute of Biomedical Materials and Engineering (SIBME), Northwestern Polytechnical University (NPU), 127 West Youyi Road, Xi'an 710072, China. E-mail: iamzftu@nwpu.edu.cn; iamslu@nwpu.edu.cn

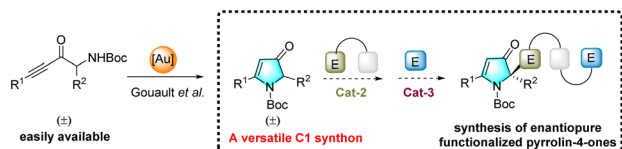
^bDepartment of Chemistry, National University of Singapore, 3 Science Drive 3, Singapore 117543, Singapore. E-mail: chmwmw@nus.edu.sg

† Electronic supplementary information (ESI) available. CCDC 2202374 and 2250756. For ESI and crystallographic data in CIF or other electronic format see DOI: <https://doi.org/10.1039/d4sc03190c>

a) A diagram of ternary catalytic reactions



b) Design plan: racemic pyrrolin-4-ones formed *in situ*: novel, versatile C1 synthon for the ternary catalysis



Scheme 1 Ternary catalytic reactions for the efficient synthesis of complex chiral molecules.



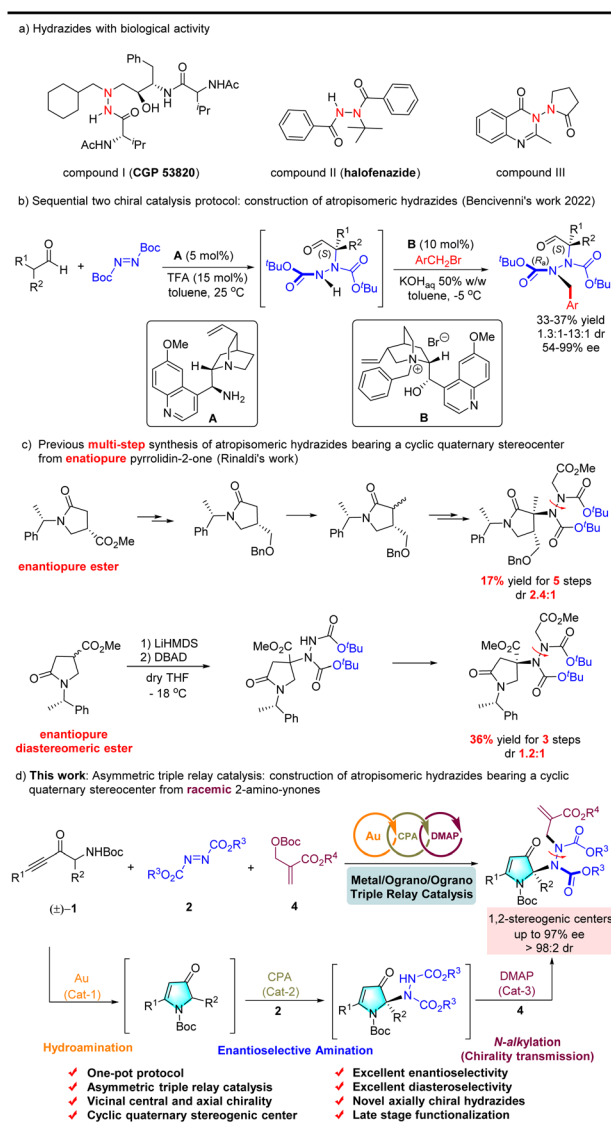
insecticides (e.g., halofenozide and derivatives; Scheme 2(a)).⁴ However, several methods for the enantioselective synthesis of N–N axially chiral heterocyclic architectures have been reported. Nonetheless, the relevant studies focused only on their atroposelective creation.⁵ Recently, the elegant catalytic enantio- and diastereoselective synthesis of axially chiral hydrazides was achieved *via* two sequential asymmetric organocatalytic cycles in one pot (see Scheme 2b).⁶ However, synthesizing enantiopure N–N axially chiral hydrazides bearing a cyclic quaternary stereocenter requires multiple steps. Rinaldi *et al.* reported two such methods. The first employs an enantiopure ester substrate to control the installation of N–N axial chirality, obtaining the desired product in 17% yield in five steps with a low dr of 2.4 : 1 (see Scheme 2c, eqn (1)).⁷ The second method employs an enantiopure diastereomeric ester to afford an N–N axially chiral product in 36% yield over three steps and a low dr of 1.2 : 1

(Scheme 2c, eqn (2)).⁸ Notably, only azo dicarboxylates with a *tert*-butyl group (excessive steric hindrance) are used as the nitrogen source in both reactions. In summary, an efficient catalytic approach for the synthesis of optically pure atropisomeric hydrazides with a wide substrate scope is yet to be developed.

To improve the field of axially chiral entities⁹ and asymmetric relay catalytic reactions,¹⁰ we examined the possibility of constructing axially chiral hydrazides through ternary catalysis. Hence, this study reports an unprecedented example of ternary catalysis that integrates gold, Brønsted chiral phosphoric acid (CPA), and an organocatalyst (DMAP), and we demonstrate its effectiveness in the highly enantioconvergent and diastereoselective construction of atropisomeric hydrazides *via* a one-pot sequence involving an intramolecular hydroamination, an intermolecular asymmetric amination, and *N*-alkylation (see Scheme 2d).

Experimental section

We initially designed the enantioconvergent synthesis of **3** by employing the dual catalysis of achiral AuCl and CPA as a starting point for studying intramolecular hydroamination, followed by asymmetric amination to facilitate the subsequent development of annulation reactions. We surveyed the reaction between racemic α -amino-ynone (**1a**) and dibenzyl azodicarboxylate (**2a**)¹¹ with AuCl¹² and CPAs¹³ *via* dual catalysis strategies.¹⁴ As listed in Table 1, various CPAs can enable the relay reaction to proceed smoothly and afford the desired product **3a** in 5–86% yield at a high level (83–88%) of ee values



Scheme 2 Bioactive molecules containing the hydrazides and synthesis of the optically active atropisomeric hydrazides bearing a cyclic quaternary stereocenter.

Table 1 Reaction condition screening^a

Entry	CPA	Solvent	Yield 3a ^b (%)	ee 3a ^c (%)
1	CPA1	Toluene	78	83
2	CPA2	Toluene	72	85
3	CPA3	Toluene	86	88
4	CPA4	Toluene	80	88
5	CPA5	Toluene	<5	—
6	CPA3	MTBE	<5	—
7	CPA3	THF	<5	—
8	CPA3	Cyclohexane	90	91
9 ^d	CPA3	Cyclohexane	90	92
10 ^e	CPA3	Cyclohexane	93	93

^a The reaction was carried out with **1a** (0.06 mmol, 1.2 equiv.), azo dicarboxylate **2a** (0.05 mmol, 1.0 equiv.), AuCl (10 mol%), CPA (5 mol%) in solvent (1 mL) under a N₂ atmosphere at 30 °C for 18 h. ^b Isolated yield of **3a** with respect to **2a**. ^c Determined by HPLC. ^d With additive 4 Å MS (50 mg). ^e With additive 5 Å MS (50 mg).



(see Table 1, entries 1–5). Hence, the common commercially available CPA3 was used as the catalyst, and the desired enantioconvergent amination **3a** was obtained in 86% yield and 88% ee (see Table 1, entry 3). Moreover, different solvents and molecular sieves were tested in the presence of CPA3 (see Table 1, entries 6–10). With the optimal choice of cyclohexane and 5 Å MS, an excellent ee of 93% was observed for **3a**.

Results and discussion

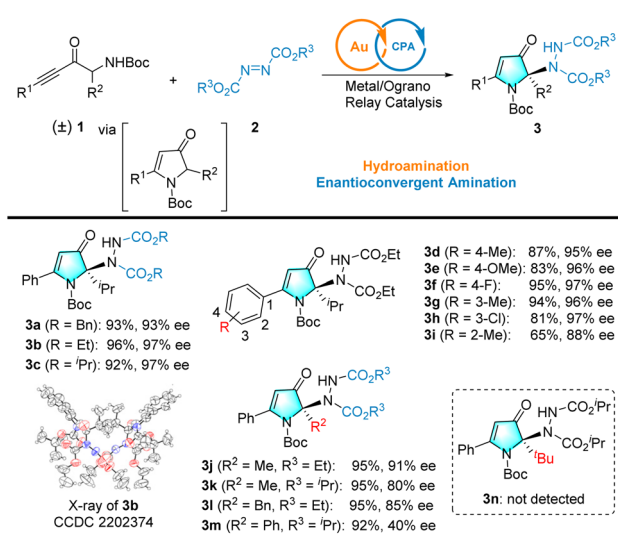
With reaction conditions optimized, we next examined the generality of the catalytic reaction (see Scheme 3), starting with a series of commercially available azodicarboxylates (*i.e.*, DEAD, DIAD, and DBAD) reacting with racemic α -amino-ynone **1a** to afford products (**3a–3c**). Good yields (92–96%) and excellent enantioselectivities (97%) of products **3b** and **3c** were obtained for ethyl and isopropyl azodicarboxylates. The absolute configuration of **3b** was unambiguously determined by single-crystal X-ray diffraction (XRD). The configurations of other products were assigned as analogies; however, when azo dicarboxylates with *tert*-butyl groups (excessive steric hindrance) were used as the nitrogen source, the target product was not observed.

Variations in racemic α -amino-ynones **1** were explored next. Notably, the reaction can tolerate a wide variety of electron-donating or -withdrawing groups at different positions of the phenyl group. Furthermore, the yields and enantioselectivities of the corresponding products **3d–3i** remained high. Alternatively, when using the less bulky racemic α -amino-ynones **1** bearing simple methyl or benzyl substituents, the reaction provided **3j–3l** in high yields and 80–91% ee. The alkyl group was replaced with an aryl group that afforded product **3m** with high yield and moderate enantioselectivity (40% ee). The R^2 group was replaced with a *tert*-butyl group, which failed to provide the desired product **3n**, presumably due to the size of the *tert*-butyl group. Fourteen additional examples are illustrated in Scheme S1 (see the ESI† for details). Consequently, this

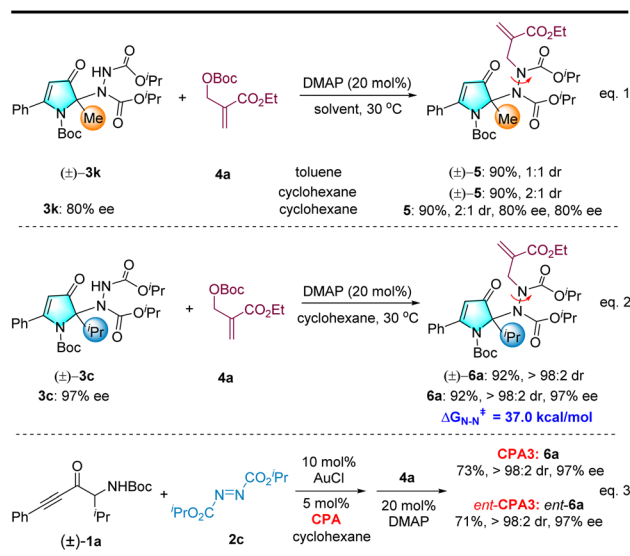
novel cascade reaction represents an atom- and step-economical approach.

We then turned our attention to the *N*-alkylation reaction of the intramolecular hydroamination/intermolecular amination reaction to create atropisomeric hydrazides (see Scheme 4).¹⁵ To our delight, the racemic **3k** underwent an *N*-alkylation reaction in the presence of the Morita–Baylis–Hillman (MBH) carbonate **4a**, achiral catalytic DMAP, and toluene to deliver an axially chiral hydrazide bearing a cyclic quaternary stereocenter **5** with 90% yield but only 1 : 1 dr (Scheme 4, eqn (1)). Nonetheless, the dr value can be improved to 2 : 1 when the solvent is switched to cyclohexane, which we used to prepare substrate **3** *via* a relay catalytic reaction. Enantioenriched **3k** was employed in the reaction, and the desired product **5** was obtained with the same enantiopurity. We speculate that the steric hindrance of the isopropyl groups may have affected diastereoselectivity. Notably, either racemic or enantiopure **3c** was used as a substrate. Fortunately, a single diastereomer **6a** was obtained at 92% yield, and high enantiopurity was retained without erosion (see Scheme 4, eqn (2)). Both CPA3 enantiomers were tested, and those corresponding to the product were obtained as single diastereomers. This result demonstrates that CPA is not effective for diastereoselectivity in *N*-alkylation with MBH carbonate (see Scheme 4, eqn (3)).

The configurational stability of this new type of N–N-linked axially chiral compound was investigated both experimentally and computationally. Heating of product (**6a**) in toluene for 72 h at 150 °C led to no erosion of diastereopurity, which was corroborated by the high rotational barrier of 37.0 kcal mol^{−1} calculated for the N–N axis at 150 °C. Notably, the cyclohexane solvent used for the *N*-alkylation reaction was the same as that used for the AuCl/CPA relay catalytic reaction. Our next goal was to create axially chiral hydrazides bearing cyclic quaternary stereocenters *via* ternary catalysis. Representative optimization studies are provided in the ESI (see Table S1†).



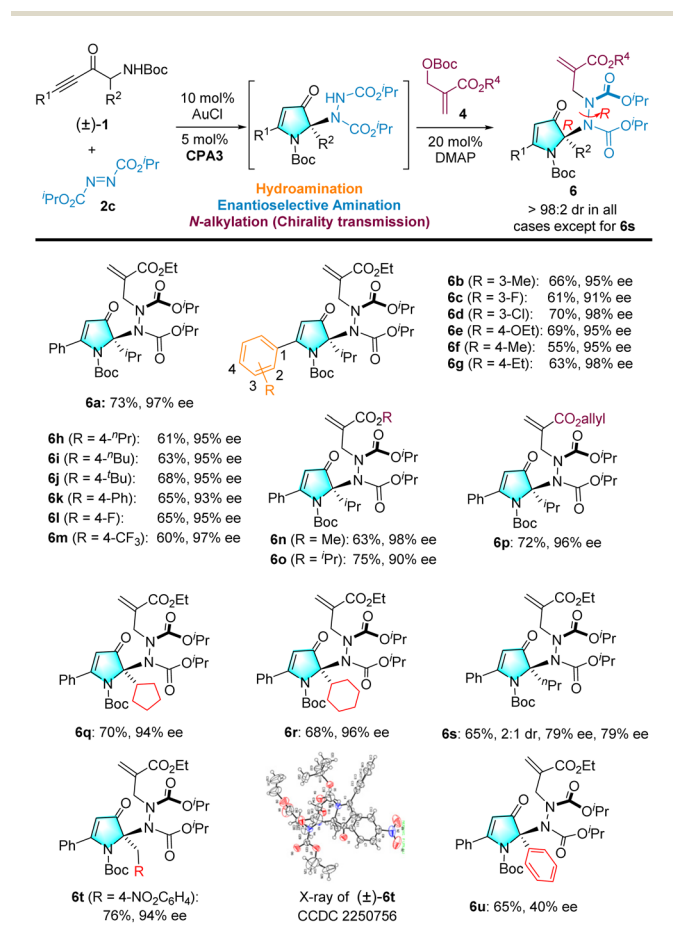
Scheme 3 Scope of gold and CPA.



Scheme 4 Investigation of axially chiral hydrazide and the effect of CPA.



Having optimized the reaction conditions, we turned to examine the generality of the ternary catalyst, by varying racemic α -amino-ynones first. A wide range of electron-donating or -withdrawing group substituents on the phenyl moiety at the 3- and 4-positions were tolerated to afford axially hydrazides **6a–6m** in good yield and uniformly excellent diastereo- and enantioselectivity (see Scheme 5). Next, different MBH carbonate ester groups were evaluated, and methyl and allyl esters gave the desired products (**6n** and **6p**) with moderate yields and excellent enantioselectivity. In contrast, bulkier isopropyl ester groups gave axially hydrazide **6o** in moderate yield, but with slightly lower enantioselectivity (90% ee). Other branched alkyl groups (*i.e.*, cyclopentyl and cyclohexyl) were introduced, and the corresponding products (**6q** and **6r**) were obtained in a high yield with excellent enantioselectivity. A linear alkyl group (t Pr) was also found to be compatible, yielding **6s** in moderate yield and enantioselectivity but with a low dr (2 : 1). The α -amino-ynones **1** bearing the 4-nitrobenzyl substituent were also tested, and the reaction afforded **6t** with 76% yield and 94% ee. The relative configuration of racemic **6t** was determined by single-crystal XRD, and the absolute configuration of the quaternary carbon stereogenic center of **6** was determined to be *R* according to the X-ray structure analysis of **3b**. To further confirm that the *R,R*-configuration product was the key experimental outcome, we compared the experimental



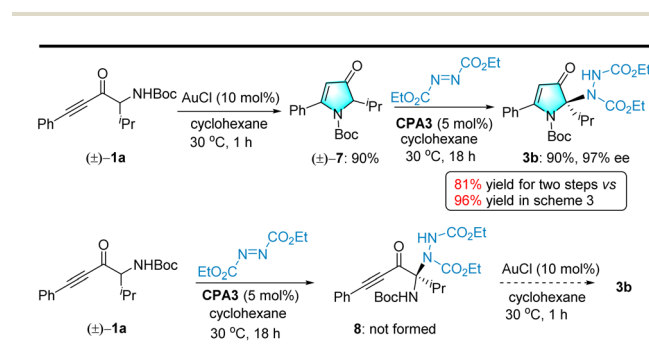
Scheme 5 Scope of the atroposelective synthesis of hydrazides.

electronic circular dichroism (ECD) spectra of enantiopure **6a** with the calculated ECD spectra of the two stereoselective products (see the ESI†). The alkyl group was replaced by a phenyl group and afforded product **6u** with high yield and moderate enantioselectivity (40% ee).

We hypothesized that two possible pathways exist for the AuCl/CPA relay catalytic reaction. Hence, to gain insights into the relay catalytic reaction pathway, control experiments were performed stepwise (see Scheme 6). First, racemic pyrrolin-4-one **7** was obtained as the product (90% yield) from racemic α -amino-ynone **1a** under the catalysis of AuCl (10 mol%) without diethyl azodicarboxylate **2a** or CPA3. Subsequently, treatment of **7** with diethyl azodicarboxylate **2a** and chiral CPA3 (5 mol%) afforded an amination product **3b** in 90% yield and 97% ee (see Scheme 6, eqn (1)). Additionally, the stepwise procedure delivered the desired products in lower two-step yields than our relay catalytic approach and efficiently avoided the loss of racemic pyrrolin-4-one intermediates during the additional purification. Alternatively, when the reaction was carried out with **1a** and diethyl azodicarboxylate **2b** in the presence of catalytic CPA3 (5 mol%), the desired product **8** was not observed (see Scheme 6, eqn (2)). These results demonstrated that the relay catalytic reaction followed the first pathway (see Scheme 6, eqn (1)).

To gain a better understanding of the reaction pathways, we monitored the kinetics of the reaction between **1a** and **2b** using ¹H NMR spectroscopy (see Scheme 7). The kinetic profiles of this reaction clearly indicated that an essentially full conversion of **1a** to the intermediate product **7** was observed within 1 h at 30 °C, which was then converted to the final product, **3b**, in a remarkably high yield. Consequently, the two catalytic reactions were identified as relays.

Based on the above results, a plausible triple-relay catalytic reaction mechanism was proposed: (1) activation of racemic α -amino-ynones (**1**) by AuCl (*via* **I**) yields intramolecular cyclization product **II**, and protonolysis of that then produces racemic pyrrolin-4-one **7**. (2) Subsequently, 3-hydroxypyrroles were formed through enolization in the presence of CPA, and the CPA catalyst activated both reactants by forming dual H-bonds with 3-hydroxypyrroles (with their 3-hydroxy group) and azodicarboxylates, which underwent an additional reaction to provide the enantioenriched amination product **3**, possessing a cyclic quaternary stereocenter, which is an enantio-determining step. (3) The first S_N² reaction was triggered by



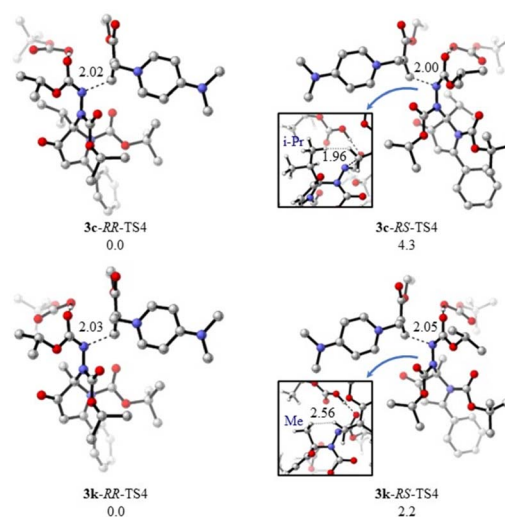
Scheme 6 Control experiments.



stereocenter **6a** with NBS at 30 °C in DCM delivered the desired product **14** in 88% yield. Additionally, the hydrolysis of **6a** at room temperature delivered free acid **15** in 84% yield (see Scheme 9(b)). Notably, in all of these transformations, excellent enantiopurity remained nearly without erosion.

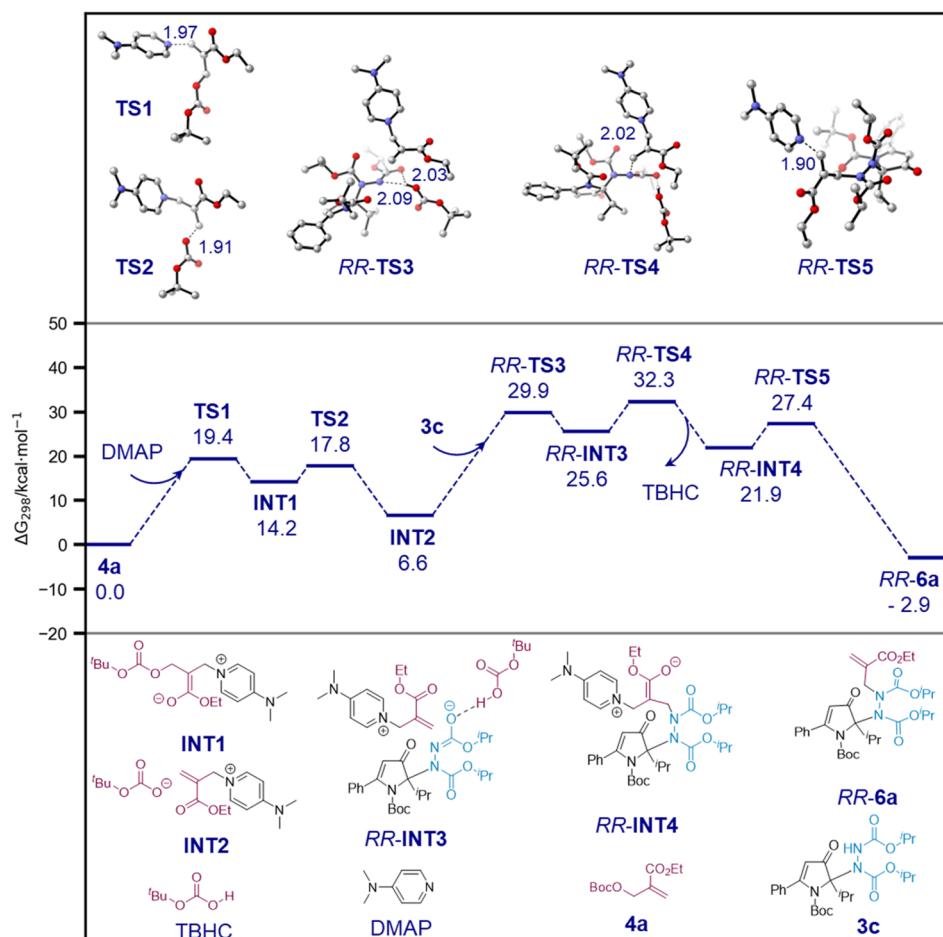
Finally, we computationally investigated the *N*-alkylation of **3c** in the presence of carbonate **4a** and DMAP to form **6a** to understand the origin of its high diastereoselectivity. Preliminary calculations demonstrated that the barrier of rotation around the N–N axis of **3c** was 22.4 kcal mol⁻¹ (see the ESI[†]), indicating that the axis was conformationally unstable and that the reaction diastereoselectivity was governed by the *N*-alkylation step. Subsequently, the entire reaction profile leading to the formation of *RR*-**6a** was calculated, and the results are illustrated in Scheme 10. The DMAP activation of **4a** was calculated as a facile process with a barrier of 19.4 kcal mol⁻¹. The generated **INT2** contained a *t*-butyl carbonate anion, which serves as a Brønsted base to deprotonate the N–H moiety of **3c** and turn it into a more potent nucleophile. The nucleophilic N–C bond formation, followed by the regeneration of the DMAP catalyst, yielded **6a**. The highest-energy step was determined to be nucleophilic N–C bond formation with a ΔG_{295} value of 32.3 kcal mol⁻¹.

We then calculated the diastereoselectivity-determining transition states for *N*-alkylation of **3c** and **3k**, and the



Scheme 11 Diastereoselectivity of *N*-alkylation of **3c** (top) and **3k** (bottom). Enclosed are rotated structures showing the steric hindrance in 3*c*-*RS*-*TS4*. ΔG_{298} values are reported in kcal mol⁻¹ and distances in Å.

optimized structures are shown in Scheme 11. Although the calculated energy differences of 4.3 and 2.2 kcal mol⁻¹ for **3c** and **3k**, respectively, would predict *dr* values much larger than those



Scheme 10 Calculated reaction profile of *N*-alkylation of **3c**. ΔG_{298} values are reported in kcal mol⁻¹ and distances in Å.



observed experimentally, there was evidence that this might be the consequence of the presence of numerous low-lying frequencies in the transition states. Hence, their treatment with quasi-harmonic approximation will lead to improved results. Furthermore, predictions based on enthalpy differences, which are less sensitive to low-lying frequencies, yielded improved results. Nevertheless, in all cases, our calculated results predicted better diastereoselectivity for **3c** than **3k**, which is in excellent agreement with the experimental results and can be attributed to the greater steric hindrance exerted by the *i*-Pr group of **3c**. A very close H–H contact of 1.96 Å was observed between the *i*-Pr group of **3c** and the C–H protons of the incoming electrophile. In comparison, the shortest H–H contact between the Me group of **3k** and the electrophile was 2.56 Å.

Conclusions

We developed a catalytic, enantioconvergent, and diastereoselective synthesis of atropisomeric hydrazides from readily available starting materials. The cascade reaction proceeded *via* ternary catalysis involving gold(I) chloride, CPA, and DMAP, with all three catalytic cycles interwoven. A variety of racemic α -amino-ynones, azodicarboxylates, and MBH carbonates were successfully assembled in one pot in good yields and with excellent regioselectivities, which delivered the products with uniformly excellent control of central and axial chirality. DFT calculations revealed the origin of diastereoselectivity. The success of this work not only provides a useful strategy for the construction of contiguous cyclic quaternary central and N–N axial chirality in one pot but also represents the first example of a catalytic synthesis of optically pure N–N atropisomers *via* ternary catalysis. The development of new catalytic processes for accessing other challenging structures with different chiralities is currently under investigation.

Data availability

The data supporting this article have been uploaded as part of the ESI.†

Author contributions

S. L. conceived the project. X. W., S.-J. W., X. X. and H. A. performed the experiments and prepared the ESI.† H. Y. performed the DFT studies. S. L., Z. T., H. Y. and M. W. W. wrote the manuscript. All authors discussed the results.

Conflicts of interest

There are no conflicts to declare.

Acknowledgements

We are grateful for the generous financial support from the Program for Young Talents of Shaanxi Province (5113200043) and the Fundamental Research Funds for Central Universities.

Notes and references

- For selected reviews, see: (a) L. F. Tietze, Domino Reactions in Organic Synthesis, *Chem. Rev.*, 1996, **96**, 115–136; (b) J. M. Lee, Y. Na, H. Han and S. Chang, Cooperative multi-catalyst systems for one-pot organic transformations, *Chem. Soc. Rev.*, 2004, **33**, 302–312; (c) J. C. Wasilke, S. J. Obrey, R. T. Baker and G. C. Bazan, Concurrent Tandem Catalysis, *Chem. Rev.*, 2005, **105**, 1001–1020; (d) Z.-H. Shao and H.-B. Zhang, Combining Transition Metal Catalysis and Organocatalysis: A Broad New Concept for Catalysis, *Chem. Soc. Rev.*, 2009, **38**, 2745–2755; (e) L. M. Am-brosini and T. H. Lambert, Multicatalysis: Advancing Synthetic Efficiency and Inspiring Discovery, *ChemCatChem*, 2010, **2**, 1373–1380; (f) D. B. Ramachary and S. Jain, Sequential one-pot combination of multi-component and multi-catalysis cascade reactions: an emerging technology in organic synthesis, *Org. Biomol. Chem.*, 2011, **9**, 1277–1300; (g) Z. T. Du and Z.-H. Shao, Combining Transition Metal Catalysis and Organocatalysis – an Update, *Chem. Soc. Rev.*, 2013, **42**, 1337–1378; (h) D.-F. Chen, Z.-Y. Han, X.-L. Zhou and L.-Z. Gong, Asymmetric Organo-catalysis Combined with Metal Catalysis: Concept, Proof of Concept, and Beyond, *Acc. Chem. Res.*, 2014, **47**, 2365–2377; (i) T. L. Lohr and T. J. Marks, Orthogonal tandem catalysis, *Nat. Chem.*, 2015, **7**, 477–482; (j) Q.-J. Liang, Y.-H. Xu and T.-P. Loh, Multi-catalyst promoted asymmetric relay reactions, *Org. Chem. Front.*, 2018, **5**, 2765–2768; (k) S. P. Sancheti, Urvashi, M. P. Shah and N. T. Patil, Ternary Catalysis: A Stepping Stone toward Multicatalysis, *ACS Catal.*, 2020, **10**, 3462–3489; (l) B. A. Arndtsen and L.-Z. Gong, *Topics in Current Chemistry Collections: Asymmetric Organocatalysis Combined with Metal Catalysis*, Springer Nature, Cham, Switzerland, 2020; (m) S. Martínez, L. Veth, B. Lainer and P. Dydio, Challenges and Opportunities in Multicatalysis, *ACS Catal.*, 2021, **11**, 3891–3915; (n) L.-Z. Gong, *Asymmetric Organo-Metal Catalysis: Concepts, Principles, and Applications*, Wiley-VCH, Weinheim, Germany, 2021; (o) D.-F. Chen and L.-Z. Gong, Organo/Transition-Metal Combined Catalysis Rejuvenates Both in Asymmetric Synthesis, *J. Am. Chem. Soc.*, 2022, **144**, 2415–2437.
- For the enantio- and diastereoselective asymmetric triple relay catalysis, see: (a) B. Simmons, A. M. Walji and D. W. C. MacMillan, Cycle-Specific Organocascade Catalysis: Application to Olefin Hydroamination, Hydro-oxidation, and Amino-oxidation, and to Natural Product Synthesis, *Angew. Chem., Int. Ed.*, 2009, **48**, 4349–4353; (b) W.-L. Yang, X.-Y. Shang, T. Ni, H. Yan, X. Luo, H. Zheng, Z. Li and W.-P. Deng, Diastereo- and Enantioselective Synthesis of Bisbenzannulated Spiroketal and Spiroaminals by Ir/Ag/Acid Ternary Catalysis, *Angew. Chem., Int. Ed.*, 2022, **61**, e202210207. For the selected enantioselective asymmetric triple relay catalysis, see: (c) X.-P. Yin, X.-P. Zeng, Y.-L. Liu, F.-M. Liao, J.-S. Yu, F. Zhou and J. Zhou, Asymmetric Triple Relay Catalysis:



- Enantioselective Synthesis of Spirocyclic Indolines through a One-Pot Process Featuring an Asymmetric 6π Electrocyclization, *Angew. Chem., Int. Ed.*, 2014, **53**, 13740–13745; (d) Z. Kang, W. Chang, X. Tian, X. Fu, W. Zhao, X. Xu, Y. Liang and W. Hu, Ternary Catalysis Enabled Three-Component Asymmetric Allylic Alkylation as a Concise Track to Chiral α,α -Disubstituted Ketones, *J. Am. Chem. Soc.*, 2021, **143**, 20818–20827.
- 3 N. Gouault, M. L. Roch, C. Cornée, M. David and P. Uriac, Synthesis of Substituted Pyrrolin-4-ones from Amino Acids in Mild Conditions *via* a Gold-Catalyzed Approach, *J. Org. Chem.*, 2009, **74**, 5614–5617.
- 4 (a) J. P. Priestley, A. Fässler, J. Rösel, M. Tintelnot-Blomley, P. Strop and M. G. Grütter, Comparative analysis of the X-ray structures of HIV-1 and HIV-2 proteases in complex with CCP 53820, a novel pseudosymmetric inhibitor, *Structure*, 1995, **3**, 381–389; (b) M. J. Mulvihill, S. H. Shaber, B. S. MacDougall, C. Ajello, B. Martinez-Teipel, R. Joseph, D. V. Nguyen, D. G. Weaver, K. Chung, A. Gusev, J. M. Wierenga and W. D. Mathis, Synthesis of Insecticidally Active Halofenozide-[(Acyloxy)alkoxy]carbonyl and (Acyloxy)alkyl Derivatives, *Synthesis*, 2002, 53–58; (c) S. Ke, T. Sun, Y. Liang and Z. Yang, Research Advance of Acylhydrazine Derivatives with Biological Activities, *Chin. J. Org. Chem.*, 2010, **30**, 1820–1830.
- 5 (a) G.-J. Mei, J. J. Wong, W. Zheng, A. A. Nangia, K. N. Houk and Y. Lu, Rational design and atroposelective synthesis of N–N axially chiral compounds, *Chem*, 2021, **7**, 2743–2757; (b) G. Centonze, C. Portolani, P. Righi and G. Bencivenni, Enantioselective Strategies for The Synthesis of N–N Atropisomers, *Angew. Chem., Int. Ed.*, 2023, **62**, e202303966; (c) J. Feng, C.-J. Lu and R.-R. Liu, Catalytic Asymmetric Synthesis of Atropisomers Featuring an Aza Axis, *Acc. Chem. Res.*, 2023, **56**, 2537–2554; (d) H.-H. Zhang, T.-Z. Li, S.-J. Liu and F. Shi, Catalytic Asymmetric Synthesis of Atropisomers Bearing Multiple Chiral Elements: An Emerging Field, *Angew. Chem., Int. Ed.*, 2023, **62**, e202311053; (e) X.-M. Wang, P. Zhang, Q. Xu, C.-Q. Guo, D.-B. Zhang, C.-J. Lu and R.-R. Liu, Enantioselective Synthesis of Nitrogen–Nitrogen Biaryl Atropisomers *via* Copper-Catalyzed Friedel–Crafts Alkylation Reaction, *J. Am. Chem. Soc.*, 2021, **143**, 15005–15010; (f) P. Zhang, Q. Xu, X.-M. Wang, J. Feng, C.-J. Lu, Y. Li and R.-R. Liu, Enantioselective Synthesis of N–N Bisindole Atropisomers, *Angew. Chem., Int. Ed.*, 2022, **61**, e202212101; (g) Y. Gao, L.-Y. Wang, T. Zhang, B.-M. Yang and Y. Zhao, Atroposelective Synthesis of 1,1'-Bipyrroles Bearing a Chiral N–N Axis: Chiral Phosphoric Acid Catalysis with Lewis Acid Induced Enantiodivergence, *Angew. Chem., Int. Ed.*, 2022, **61**, e202200371; (h) K.-W. Chen, Z.-H. Chen, S. Yang, S.-F. Wu, Y.-C. Zhang and F. Shi, Organocatalytic Atroposelective Synthesis of N–N Axially Chiral Indoles and Pyrroles by De Novo Ring Formation, *Angew. Chem., Int. Ed.*, 2022, **61**(No), e202116829; (i) W. Lin, Q. Zhao, Y. Li, M. Pan, C. Yang, G. Yang and X. Li, Asymmetric Synthesis of N–N Axially Chiral Compounds *via* Organocatalytic Atroposelective N-Acylation, *Chem. Sci.*, 2022, **13**, 141–148; (j) Q. Xu, H. Zhang, F.-B. Ge, X.-M. Wang, P. Zhang, C.-J. Lu and R.-R. Liu, Cu(I)-Catalyzed Asymmetric Arylation of Pyrroles with Diaryliodonium Salts toward the Synthesis of N–N Atropisomers, *Org. Lett.*, 2022, **24**, 3138–3143; (k) L.-Y. Pu, Y.-J. Zhang, W. Liu and F. Teng, Chiral Phosphoric Acid-Catalyzed Dual-Ring Formation for Enantioselective Construction of N–N Axially Chiral 3,3'-Bisquinazolinones, *Chem. Commun.*, 2022, **58**, 13131–13134; (l) V. Hutskalova and C. Sparr, Control over Stereogenic N–N Axes by Pd-Catalyzed 5-endo-Hydroaminocyclizations, *Synthesis*, 2023, **55**, 1770–1782; (m) Z.-H. Chen, T.-Z. Li, N.-Y. Wang, X.-F. Ma, S.-F. Ni, Y.-C. Zhang and F. Shi, Organocatalytic Enantioselective Synthesis of Axially Chiral N,N'-Bisindoles, *Angew. Chem., Int. Ed.*, 2023, **62**, e202300419; (n) L.-Y. Wang, J. Miao, Y. Zhao and B.-M. Yang, Chiral Acid-Catalyzed Atroposelective Indolization Enables Access to 1,1'-Indole-Pyrroles and Bisindoles Bearing a Chiral N–N Axis, *Org. Lett.*, 2023, **25**, 1553–1557; (o) W. Yao, C.-J. Lu, L.-W. Zhan, Y. Wu, J. Feng and R.-R. Liu, Enantioselective Synthesis of N–N Atropisomers by Palladium-Catalyzed C–H Functionalization of Pyrroles, *Angew. Chem., Int. Ed.*, 2023, **62**, e202218871; (p) S.-Y. Yin, Q. Zhou, C.-X. Liu, Q. Gu and S.-L. You, Enantioselective Synthesis of N–N Biaryl Atropisomers through Iridium(I)-Catalyzed C–H Alkylation with Acrylates, *Angew. Chem., Int. Ed.*, 2023, **62**, e202305067; (q) K. Balanna, S. Barik, S. Barik, S. Shee, N. Manoj, R. G. Gonnade and A. T. Biju, N-Heterocyclic Carbene-Catalyzed Atroposelective Synthesis of N–N Axially Chiral 3-Amino Quinazolinones, *ACS Catal.*, 2023, **13**, 8752–8759; (r) C. Wang and J. Sun, Atroposelective Synthesis of N–N Axially Chiral Bipyrroles *via* Rhodium-Catalyzed C–H Insertion Reaction, *Org. Lett.*, 2023, **25**, 4808–4812; (s) X. Zhu, H. Wu, Y. Wang, G. Huang, F. Wang and X. Li, Rhodium-Catalyzed Annulative Approach to N–N Axially Chiral Biaryls *via* C–H Activation and Dynamic Kinetic Transformation, *Chem. Sci.*, 2023, **14**, 8564–8569; (t) Y. Wang, X. Zhu, D. Pan, J. Jing, F. Wang, R. Mi, G. Huang and X. Li, Rhodium-catalyzed enantioselective and diastereodivergent access to diaxially chiral heterocycles, *Nat. Commun.*, 2023, **14**, 4661; (u) T. Li, L. Shi, X. Wang, C. Yang, D. Yang, M.-P. Song and J.-L. Niu, Cobalt-catalyzed atroposelective C–H activation/annulation to access N–N axially chiral frameworks, *Nat. Commun.*, 2023, **14**, 5271; (v) C.-S. Wang, Q. Xiong, H. Xu, H.-R. Yang, T. Dang, X.-Q. Dong and C.-J. Wang, Organocatalytic Atroposelective Synthesis of Axially Chiral N,N'-Pyrroloindoles *via* De Novo Indole Formation, *Chem. Sci.*, 2023, **14**, 12091–12097; (w) Q. Huang, Y. Li, C. Yang, W. Wu, J. Hai and X. Li, Atroposelective synthesis of N–N axially chiral pyrrolyl(aza)-quinolinone by de novo ring formation, *Org. Chem. Front.*, 2024, **11**, 726–734; (x) F.-B. Ge, Q.-K. Yin, C.-J. Lu, X. Xuan, J. Feng and R.-R. Liu, Enantioselective Synthesis of Benzimidazole Atropisomers Featuring a N–N Axis, *Chin. J. Chem.*, 2024, **42**, 711–718; (y) C. Song, C. Pang, Y. Deng, H. Cai, X. Gan and Y. R. Chi, Catalytic N-Acylation for Access to N–N Atropisomeric N-



- Aminoindoles: Choice of Acylation Reagents and Mechanistic Insights, *ACS Catal.*, 2024, **14**, 6926–6935; (z) S. S. Ranganathappa, B. S. Dehury, G. K. Singh, S. Shee and A. T. Biju, Atroposelective Synthesis of N–N Axially Chiral Indoles and Pyrroles via NHC-Catalyzed Diastereoselective (3 + 3) Annulation Strategy, *ACS Catal.*, 2024, **14**, 6965–6972.
- 6 C. Portolani, G. Centonze, S. Luciani, A. Pellegrini, P. Righi, A. Mazzanti, A. Ciogli, A. Sorato and G. Bencivenni, Synthesis of Atropisomeric Hydrazides by One-Pot Sequential Enantioselective and Diastereoselective Catalysis, *Angew. Chem., Int. Ed.*, 2022, **61**, e202209895.
- 7 P. Amabili, A. Amici, A. Civitavecchia, B. Maggiore, M. Orena, S. Rinaldi and A. Tolomelli, Highly stable atropisomers by electrophilic amination of a chiral γ -lactam within the synthesis of an elusive conformationally restricted analogue of α -methylhomoserine, *Amino Acid*, 2016, **48**, 461–478.
- 8 P. Amabili, A. Amici, G. Campisi, G. Guerra, M. Monari, M. Orena, F. Piccinelli, S. Rinaldi and A. Tolomelli, Synthesis of Enantiopure Isosteres of Amino Acids Containing a Quaternary Stereocenter: Experimental and Computational Evaluation of a Novel Class of Atropisomers, *Eur. J. Org. Chem.*, 2018, 6524–6536.
- 9 (a) S.-C. Zhang, S. Liu, X. Wang, S.-J. Wang, H. Yang, L. Li, B. Yang, M. W. Wong, Y. Zhao and S. Lu, Enantioselective Access to Triaryl-2-pyrone with Monoaxial or Contiguous C–C Diaxes via Oxidative NHC Catalysis, *ACS Catal.*, 2023, **13**, 2565–2575; (b) S.-J. Wang, X. Wang, X. Xin, S. Zhang, H. Yang, M. W. Wong and S. Lu, Organocatalytic diastereo- and atroposelective construction of N–N axially chiral pyrroles and indoles, *Nat. Commun.*, 2024, **15**, 518; (c) X. Wang, S. Zhang, S.-J. Wang, H. An, X. Xin, H. Lin, Z. Tu and S. Lu, An Assembly of Pyrano[3,2-*b*]indol-2-ones via NHC-Catalyzed [3 + 3] Annulation of Indolin-3-ones with Ynals, *Chin. J. Chem.*, 2024, **42**, 1487–1492.
- 10 J. Jiang, X. Wang, S. Liu, S. Zhang, B. Yang, Y. Zhao and S. Lu, Enantioselective Cascade Annulation of α -Amino-ynones and Enals Enabled by Gold and Oxidative NHC Relay Catalysis, *Angew. Chem., Int. Ed.*, 2022, **61**, e202115464.
- 11 (a) S. Yarlagadda, B. Ramesh, C. R. Reddy, L. Srinivas, B. Sridhar and B. V. S. Reddy, Organocatalytic Enantioselective Amination of 2-Substituted Indolin-3-ones: A Strategy for the Synthesis of Chiral α -Hydrazino Esters, *Org. Lett.*, 2017, **19**, 170–173; (b) J. Guo, Z.-H. Lin, K.-B. Chen, Y. Xie, A. S. C. Chan, J. Weng and G. Lu, Asymmetric amination of 2-substituted indolin-3-ones catalyzed by natural cinchona alkaloids, *Org. Chem. Front.*, 2017, **4**, 1400–1406; (c) X. Kong, Q. Liu, Y. Chen, W. Wang, H.-F. Chen, W. Wang, S. Zhang, X. Chen and Z.-Y. Cao, Direct electrochemical synthesis of arenesulfonyl fluorides from nitroarenes: a dramatic ionic liquid effect, *Green Chem.*, 2024, **26**, 3435–3440.
- 12 For selected recent reviews on gold chemistry, see: (a) M. Bandini, Gold-catalyzed decorations of arenes and heteroarenes with C–C multiple bonds, *Chem. Soc. Rev.*, 2011, **40**, 1358–1367; (b) A. Corma, A. Leyva-Pérez and M. J. Sabater, Gold-Catalyzed Carbon–Heteroatom Bond-Forming Reactions, *Chem. Rev.*, 2011, **111**, 1657–1712; (c) A. S. K. Hashmi and M. Rudolph, Gold catalysis in total synthesis—an update, *Chem. Soc. Rev.*, 2012, **41**, 2448–2462; (d) L. Liu and G. B. Hammond, Recent advances in the isolation and reactivity of organogold complexes, *Chem. Soc. Rev.*, 2012, **41**, 3129–3139; (e) A. S. K. Hashmi, Dual Gold Catalysis, *Acc. Chem. Res.*, 2014, **47**, 864–876; (f) L. Zhang, A Non-Diazo Approach to α -Oxo Gold Carbenes via Gold-Catalyzed Alkyne Oxidation, *Acc. Chem. Res.*, 2014, **47**, 877–888; (g) C. Obradors and A. M. Echavarren, Gold-Catalyzed Rearrangements and Beyond, *Acc. Chem. Res.*, 2014, **47**, 902–912; (h) D. Qian and J. Zhang, Gold-catalyzed cyclopropanation reactions using a carbenoid precursor toolbox, *Chem. Soc. Rev.*, 2015, **44**, 677–698; (i) W. Zi and F. D. Toste, Recent advances in enantioselective gold catalysis, *Chem. Soc. Rev.*, 2016, **45**, 4567–4589; (j) A. Fgrstner, Gold Catalysis for Heterocyclic Chemistry: A Representative Case Study on Pyrone Natural Products, *Angew. Chem., Int. Ed.*, 2018, **57**, 4215–4233; (k) F.-L. Hong and L.-W. Ye, Transition Metal-Catalyzed Tandem Reactions of Ynamides for Divergent N-Heterocycle Synthesis, *Acc. Chem. Res.*, 2020, **53**, 2003–2019; (l) D. Campeau, D. F. León Rayo, A. Mansour, K. Muratov and F. Gagosz, Gold-Catalyzed Reactions of Specially Activated Alkynes, Allenes, and Alkenes, *Chem. Rev.*, 2021, **121**, 8756–8867; (m) Z. Zheng, X. Ma, X. Cheng, K. Zhao, K. Gutman, T. Li and L. Zhang, Homogeneous Gold-Catalyzed Oxidation Reactions, *Chem. Rev.*, 2021, **121**, 8979–9038.
- 13 For reviews of CPAs, see: (a) T. Akiyama, Stronger brønsted acids, *Chem. Rev.*, 2007, **107**, 5744–5758; (b) M. Terada, Binaphthol derived phosphoric acid as a versatile catalyst for enantioselective carbon–carbon bond forming reactions, *Chem. Commun.*, 2008, 4097–4112; (c) M. Terada, Chiral phosphoric acids as versatile catalysts for enantioselective transformations, *Synthesis*, 2010, 1929–1982; (d) M. Rueping, A. Kuenkel and I. Atodiresei, Chiral Brønsted acids in enantioselective carbonyl activations—activation modes and applications, *Chem. Soc. Rev.*, 2011, **40**, 4539–4549; (e) J. Yu, F. Shi and L.-Z. Gong, Brønsted-Acid-Catalyzed Asymmetric Multicomponent Reactions for the Facile Synthesis of Highly Enantioenriched Structurally Diverse Nitrogenous Heterocycles, *Acc. Chem. Res.*, 2011, **44**, 1156–1171; (f) D. Parmar, E. Sugiono, S. Raja and M. Rueping, Complete Field Guide to Asymmetric BINOL-Phosphate Derived Brønsted Acid and Metal Catalysis: History and Classification by Mode of Activation; Brønsted Acidity, Hydrogen Bonding, Ion Pairing, and Metal Phosphates, *Chem. Rev.*, 2014, **114**, 9047–9153; (g) D. Parmar, E. Sugiono, S. Raja and M. Rueping, Addition and Correction to Complete Field Guide to Asymmetric BINOL-Phosphate Derived Brønsted Acid and Metal Catalysis: History and Classification by Mode of Activation; Brønsted Acidity, Hydrogen Bonding, Ion Pairing, and Metal Phosphates, *Chem. Rev.*, 2017, **117**, 10608–10620; (h) Z.-L. Xia, Q.-F. Xu, C. Zheng and S.-L. You, Chiral phosphoric acid-catalyzed asymmetric dearomatization reactions, *Chem. Soc. Rev.*, 2020, **49**, 286–300; (i) S. Li,



- S.-H. Xiang and B. Tan, Chiral Phosphoric Acid Creates Promising Opportunities for Enantioselective Photoredox Catalysis, *Chin. J. Chem.*, 2020, **38**, 213–214; (j) X. Lin, L. Wang, Z. Han and Z. Chen, Chiral Spirocyclic Phosphoric Acids and Their Growing Applications, *Chin. J. Chem.*, 2021, **39**, 802–824.
- 14 For a review on the gold/CPA dual asymmetric catalysis reaction: P.-S. Wang, D.-F. Chen and L.-Z. Gong, Recent Progress in Asymmetric Relay Catalysis of Metal Complex with Chiral Phosphoric Acid, *Top. Curr. Chem.*, 2020, **378**, 9. For gold(I)/CPA relay catalysis, see: Z.-Y. Han, H. Xiao, X.-H. Chen and L.-Z. Gong, Consecutive Intramolecular Hydroamination/Asymmetric Transfer Hydrogenation under Relay Catalysis of an Achiral Gold Complex/Chiral Brønsted Acid Binary System, *J. Am. Chem. Soc.*, 2009, **131**, 9182–9183; M. E. Muratore, C. A. Holloway, A. W. Pilling, R. I. Storer, G. Trevitt and D. J. Dixon, Enantioselective Brønsted Acid-Catalyzed N-Acyliminium Cyclization Cascades, *J. Am. Chem. Soc.*, 2009, **131**, 10796–10797; Z.-Y. Han, D.-F. Chen, Y.-Y. Wang, R. Guo, P.-S. Wang, C. Wang and L.-Z. Gong, Hybrid Metal/Organo Relay Catalysis Enables Enynes To Be Latent Dienes for Asymmetric Diels–Alder Reaction, *J. Am. Chem. Soc.*, 2012, **134**, 6532–6535; H. Wu, Y.-P. He and L.-Z. Gong, Direct Access to Enantioenriched Spiroacetals through Asymmetric Relay Catalytic Three-Component Reaction, *Org. Lett.*, 2013, **15**, 460–463; F. Zhao, N. Li, Y.-F. Zhu and Z.-Y. Han, Enantioselective Construction of Functionalized Tetrahydrocarbazoles Enabled by Asymmetric Relay Catalysis of Gold Complex and Chiral Brønsted Acid, *Org. Lett.*, 2016, **18**, 1506–1509; H. Wei, M. Bao, K. Dong, L. Qiu, B. Wu, W. Hu and X. Xu, Enantioselective Oxidative Cyclization/Mannich Addition Enabled by Gold(I)/Chiral Phosphoric Acid Cooperative Catalysis, *Angew. Chem., Int. Ed.*, 2018, **57**, 17200–17204; S. Zhou, X. Liu, W. Hu, Z. Ke and X. Xu, Enantioselective Oxidative Multi-Functionalization of Terminal Alkynes with Nitrones and Alcohols for Expedient Assembly of Chiral α -Alkoxy- β -amino-ketones, *J. Am. Chem. Soc.*, 2021, **143**, 14703–14711; X.-S. Liu, Z. Tang, Z.-Y. Si, Z. Zhang, L. Zhao and L. Liu, Enantioselective *para*-C(sp²)-H Functionalization of Alkyl Benzene Derivatives *via* Cooperative Catalysis of Gold/Chiral Brønsted Acid, *Angew. Chem., Int. Ed.*, 2022, **61**, e202208874.
- 15 S. Lu, S. V. H. Ng, K. Lovato, J.-Y. Ong, S. B. Poh, X. Q. Ng, L. Kürti and Y. Zhao, Practical access to axially chiral sulfonamides and biaryl amino phenols *via* organocatalytic atroposelective *N*-alkylation, *Nat. Commun.*, 2019, **10**, 3061.
- 16 (a) J. S. Moore, Shape-Persistent Molecular Architectures of Nanoscale Dimension, *Acc. Chem. Res.*, 1997, **30**, 402–413; (b) A. D. Finke, D. E. Gross, A. Han and J. S. Moore, Engineering Solid-State Morphologies in Carbazole–Ethyne Macrocycles, *J. Am. Chem. Soc.*, 2011, **133**, 14063–14070.

